Polymorphism in 3-methyl-4-methoxy-4′-nitrostilbene (MMONS), a highly active NLO material†

Parthapratim Munshi, Brian W. Skelton, Joshua J. McKinnon and Mark A. Spackman*

During crystallization experiments two new polymorphs of the highly-active organic nonlinear optical (NLO) material 3-methyl-4-methoxy-4′-nitrostilbene (MMONS) have been discovered. Crystallization conditions of all three polymorphs and their characterization *via* crystal structure determination from single crystal X-ray diffraction data at 100 K have been discussed in detail. Two of the polymorphs exhibit different conformations, while a third polymorph incorporates both conformers as well as disorder. Comparisons between various types of intermolecular contacts in these three polymorphic forms have been quantified *via* Hirshfeld surface analysis.

Introduction

Because of their large second-order optical nonlinearities, the ability to tailor their properties *via* appropriate synthetic approaches, and their ready incorporation into structures such as crystals, thin films and poled polymers, several families of organic molecules have been the focus of considerable attention as potential nonlinear optical (NLO) materials.[1] One such family comprises substituted stilbenes, azobenzenes, their salts and co-crystals. Second-harmonic generation (SHG) results were reported for a range of substituted stilbenes in 1988,[2] and powder SHG efficiencies of as much as 90 and 300 times that of urea were observed for 4-methoxy-4′-nitro-stilbene (MONS) and 1-(4-nitrophenyl)-2-(4-methoxyphenyl)-1-cyanoethylene (CMONS), respectively. In the following year the preparation and crystal structure of MMONS (3-methyl-4-methoxy-4′-nitrostilbene) were reported,[3] with a significantly higher SHG efficiency (1250× urea). The ability to grow large single crystals of MMONS has resulted in a number of studies of its properties, including linear, nonlinear and electro-optic properties of the crystal,[4] powder,[5] and thin films,[6] dipole moment and isotropic (hyper)polarizabilities in solution,[7] infrared absorption edge,[8] and crystal growth[9,10] and thin film fabrication.[11] Thus, MMONS is known to have a large (but unexceptional) dipole moment of 5.2 D, and its crystals are orange, highly birefringent, and belong to the polar noncentrosymmetric space group *Aba*2.

MMONS
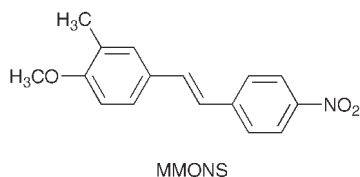
We are currently undertaking a study of the electron distributions of organic NLO molecular crystals, with a focus on wavefunction fitting to estimate in-crystal effective polarizabilities and hyperpolarizabilities from highly-accurate X-ray diffraction data.[12] The crystal structure of MMONS has been reported twice on the basis of single crystal diffraction data,[3,13] and once from powder diffraction data,[14] and all structure determinations are in essential agreement. However, as part of our study we have synthesized MMONS and have discovered two new polymorphs during relatively straightforward crystallization experiments. In hindsight this was probably not a surprising outcome, as the original study on substituted stilbenes commented that "we also observe that polymorphism is common in this group of molecules".[2] Those authors reported that SHG efficiencies for CMONS depended greatly on the crystallization conditions, with values ranging from 300× urea (for growth from ethyl acetate) to 0.15× urea (for growth from dioxane); for MONS SHG efficiencies were found to be 90× urea (for growth from ethyl acetate) but only 0.6× urea (for growth from dioxane). They also noted that "several polymorphs of CMONS and MONS are highly luminescent while others are not". The crystalline polymorphism of CMONS has recently been confirmed by Vrcelj *et al.*,[15] who reported single crystal structures for three polymorphs of the *trans* isomer. Those authors also commented on the differences between the pharmaceutical industry, where polymorph screening and characterisation is of paramount importance,[16] and the area of NLO materials, where such screening is still uncommon. Although crystalline polymorphism in MONS appears not to have been investigated, the crystal structures of three polymorphs of MOHNS (4-hydroxy-3-methoxy-4′-nitrostilbene)‡ have been reported by Gleixner *et al.*[17] Along with recent reports of new polymorphs of other NLO materials,[18] our serendipitous discovery of two new polymorphs of MMONS, for which there have been so many studies of crystal

School of Biomedical, Biomolecular and Chemical Sciences, University of Western Australia, Crawley, W.A. 6009, Australia.
E-mail: mark.spackman@uwa.edu.au; Fax: +61 8 6488 1005;
Tel: +61 8 6488 3140
† CCDC reference numbers 658143–658145. For crystallographic data in CIF or other electronic format see DOI: 10.1039/b712869j

‡ There is inconsistency in the literature in the use of the abbreviations MOHNS and HMONS. Ref. 17 refers to 3-methoxy-4-hydroxy-4′-nitrostilbene as HMONS, but in ref. 35 it is referred to as MOHNS, while HMONS is used to refer to 3-hydroxy-4-methoxy-4′-nitrostilbene, the crystal structure of which has been reported by Li and Su.[36]

structure and crystal growth over nearly two decades, serves to further underline the need for more detailed and systematic investigations of polymorphism in all materials pursued for NLO applications, as previously emphasized by Gleixner *et al.*[17]

Herein we report the results of crystallization experiments and the characterization of all three polymorphs of MMONS *via* crystal structure determination from single crystal X-ray diffraction data collected at 100 K. Two of the polymorphs exhibit different conformations, while a third polymorph incorporates both conformers as well as disorder. As such, these structures pose a challenge to any method that attempts to distil similarities and differences, and for that purpose we exploit the tools we have developed based on Hirshfeld surfaces and fingerprint plots,[19] in particular the d_{norm} property and quantitative breakdown of surfaces into contributions from particular atom–atom contacts, as described recently.[20] We also compare experimentally observed geometries for the two molecular conformations with results from *ab initio* geometry optimizations.

Results and discussion

MMONS was synthesised as described in the literature.[3] Attempts to grow single crystals from a mixture of chloroform and ethanol, at both ambient temperature and at 5–10 °C, as reported earlier,[3] resulted in several yellow crystals of block type, and suitable for X-ray diffraction studies.§ Surprisingly, cell-checking experiments on these crystals revealed a new form (which we label MMONS-2) with entirely different cell parameters from the original known form (which we now denote MMONS-1).[13] Further efforts were made to grow single crystals of the original form using combinations of various solvents and different conditions (Table 1). These crystallization experiments yielded yet another form (MMONS-3) which also crystallizes as block type, but darker yellow in colour, and from the slow evaporation of a mixture of chloroform and hexane at ambient temperature. We were eventually successful in growing single crystals of MMONS-1 from the slow evaporation of a saturated methanol/hexane solution at ambient temperature. These crystals are prismatic in shape but again dark yellow in colour. During the preparation of this manuscript, we came across the study by Hong *et al.* on crystal growth of MMONS from various solvents *via* slow evaporation at room temperature.[10] Although

§ **Crystal/refinement details:** $C_{16}H_{15}NO_3$, $M = 269.29$, $T = 100(2)$ K; (a) **MMONS-1**, orthorhombic, $Aba2$, $Z = 8$, $F(000) = 1136$, $a = 15.4037(3)$, $b = 13.4121(2)$, $c = 13.2831(2)$ Å, $V = 2744.23(8)$ Å^3; $D_c = 1.304$ g cm^{-3}; $\sin(\theta/\lambda)_{max} = 0.6497$, N(unique) = 1679 (merged from 17023, $R_{int} = 0.0295$), N_o ($I > 2\sigma(I)$) = 1521; $R = 0.0373$, $wR2 = 0.1050$, GOF = 1.074; $|\Delta\rho|_{max} = 0.23$ e Å^{-3}. (b) **MMONS-2**, monoclinic, $P2_1$, $Z = 4$, $F(000) = 568$, $a = 11.8890(2)$, $b = 7.4118(1)$, $c = 15.6083(2)$ Å, $b = 103.661(2)°$, $V = 1336.48(4)$ Å^3; $D_c = 1.338$ g cm^{-3}; $\sin(\theta/\lambda)_{max} = 0.7044$, N(unique) = 3307 (merged from 16957, $R_{int} = 0.0218$), N_o ($I > 2\sigma(I)$) = 2772; $R = 0.0430$, $wR2 = 0.1309$, GOF = 1.085; $|\Delta\rho|_{max} = 0.26$ e Å^{-3}. (c) **MMONS-3**, orthorhombic, $Pbca$, $Z = 8$, $F(000) = 1136$, $a = 7.2691(5)$, $b = 14.0308(12)$, $c = 26.229(2)$ Å, $V = 2675.1(4)$ Å^3; $D_c = 1.337$ g cm^{-3}; $\sin(\theta/\lambda)_{max} = 0.6168$, N(unique) = 2630 (merged from 13103, $R_{int} = 0.0556$), N_o ($I > 2\sigma(I)$) = 1702; $R = 0.0551$, $wR2 = 0.1231$, GOF = 1.044; $|\Delta\rho|_{max} = 0.19$ e Å^{-3}. CCDC reference numbers 658143–658145. For crystallographic data in CIF format see DOI: 10.1039/b712869j

Table 1 Details of crystallization experiments

Solvent(s)	Condition	Crystal habit and quality	Colour	Form
Chloroform/ethanol	LT	**block; good**	**yellow**	**2**
	RT	block; fair	yellow	2
Chloroform/hexane	LT	rod, plate; fair	yellow	2
	RT	**block; good**	**dark yellow**	**3**
Acetone	LT	—	—	—
	RT	poor	—	—
Acetone/hexane	LT	poor	—	—
	RT	—	—	—
Acetonitrile	LT	fibre; poor	—	—
	RT	poor	—	—
Toluene	LT	—	—	—
	RT	—	—	—
Chloroform	LT	poor	—	—
	RT	—	—	—
Chloroform/ethyl acetate	LT	poor	—	—
	RT	—	—	—
Ethanol	LT	—	—	—
	RT	prismatic; fair	dark yellow	1
Ethanol/hexane	LT	prismatic; good	dark yellow	1
	RT	prismatic; fair	dark yellow	1
Methanol	LT	block; good	dark yellow	3
	RT	block; good	dark yellow	3
Methanol/hexane	LT	prismatic; fair	dark yellow	1
	RT	**prismatic; good**	**dark yellow**	**1**

^{a} LT = low temperature (5–10 °C), RT = room temperature (20–23 °C). X-ray diffraction studies based on crystals from experiments highlighted in bold.

a wide range of habits and varying quality of crystals were observed in their experiments, no polymorphic forms were identified.

MMONS-1

This previously known form crystallizes in the polar non-centrosymmetric space group $Aba2$ with $Z = 8$. Taking into account the effects of cell contraction, the present cell constants obtained at 100 K are consistent with those from the earlier studies.[3,13,14]¶ An ORTEP view of the molecule along with the atom-numbering scheme is shown in Fig. 1. The molecular geometry of the present structure determined at 100 K is comparable with the earlier structure reported at 291 K.[13] Relevant quantities are the central C=C bond length, the torsion angles associated with the bonds connecting the two phenyl rings and the dihedral angle between the plane of these rings, and those calculated from the present crystal geometry are compared with the previous results from Suh *et al.*,[13] and with the optimised *ab initio* results in Table 2. The molecule in MMONS-1 is almost planar (Fig. 2), with a dihedral angle of 6.2°; in contrast, the molecule becomes non-planar on geometry optimization, with a dihedral angle of 43.0° (Table 2). The molecules pack in the crystal lattice in a fashion that generates an overall herringbone-like structure, as shown in Fig. 3a. In the projection down c the structure is seen to comprise intersecting sheets of molecules with close C–H⋯O contacts between the O(nitro) atoms and H3 and

¶ Ref. 3 reports $T = 70$ °C for the crystal structure determination, but the CCDC entry (JAVCEO) notes that this should probably be 70 K. However, the cell dimensions reported in ref. 3 ($a = 15.584(1)$, $b = 13.463(1)$, $c = 13.299(3)$ Å) suggest $100 < T < 291$ K for that structure.
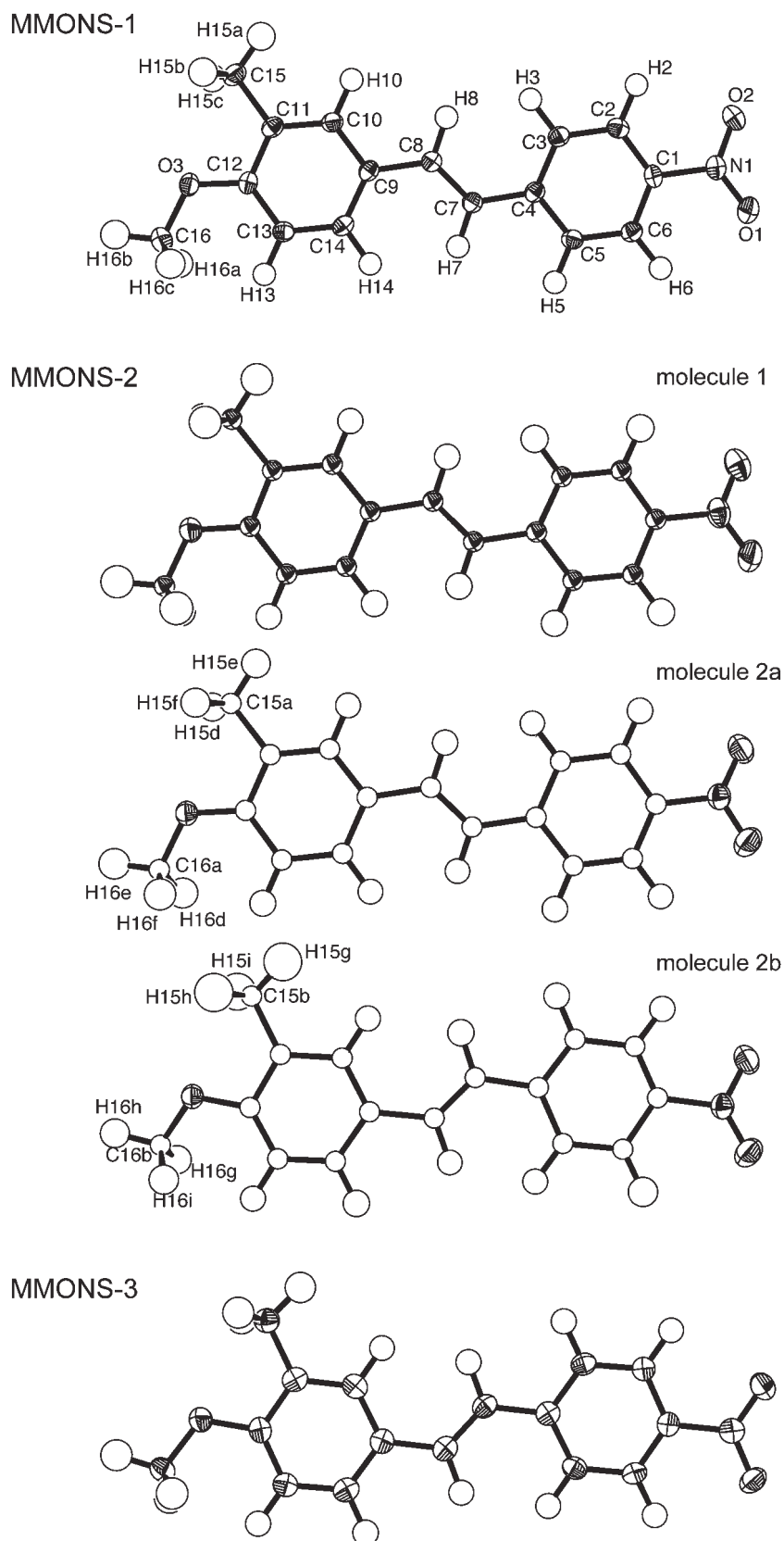
Fig. 1 ORTEP[21] views of molecules in MMONS-1, MMONS-2 and MMONS-3, showing the atom labelling scheme; common labels are shown only for MMONS-1. Ellipsoids are drawn with 50% probability level.

Table 2 Central C=C bond distance (Å), torsion angles (°) and the dihedral angle between the two phenyl rings for molecules in the three MMONS polymorphs, and for *ab initio* optimized structures

| | MMONS-1 | | MMONS-2 | | | MMONS-3 | *Ab initio* results | |
	Present work	Suh *et al.*[13]	Molecule 1	Molecule 2a	Molecule 2b		MMONS-1[a]	MMONS-3[a]
C7=C8	1.341(3)	1.315(8)	1.334(3)	1.322(5)	1.336(10)	1.338(3)	1.329	1.329
C3–C4–C7=C8	−0.8(4)	1.5(8)	−1.0(4)	−8.4(6)	−179.7(8)	−173.1(2)	−22.5	158.0
C5–C4–C7=C8	178.9(2)	−179.8(13)	−179.1(3)	170.4(4)	−0.9(12)	4.6(3)	158.0	−22.6
C4–C7=C8–C9	−178.7(2)	−179.1(15)	179.9(2)	179.4(4)	179.0(8)	176.4(2)	179.8	−179.9
C7=C8–C9–C10	−174.0(2)	−175.9(13)	170.0(2)	−170.0(4)	1.2(3)	3.6(3)	159.7	−15.4
C7=C8–C9–C14	6.9(4)	4.8(9)	−8.8(4)	8.6(6)	175.6(9)	−174.4(2)	−20.8	164.9
Dihedral angle	6.2(1)	5.9(3)	9.7(1)	2.1(1)	4.1(3)	12.8(1)	43.0	37.5

[a] Results of geometry optimizations at the HF/6-31G(d,p) level, with initial geometries from MMONS-1 and MMONS-3.
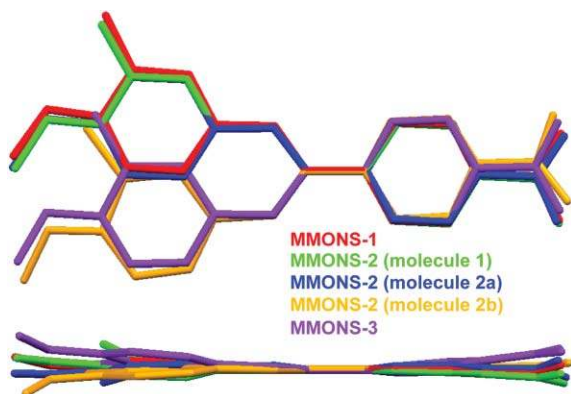

Fig. 2 Mercury[28] overlay of MMONS molecules in the three polymorphs showing differences in molecular geometry and conformation. The upper view is from above the C4–C7 bond, and the lower view is perpendicular to this.

H8 [H3···O1 = 2.59 Å, H3···O2 = 2.52 Å, H8···O2 = 2.36 Å] (Fig. 3b). Intersection of the molecular sheets results in bifurcated C–H···O contacts at the methoxy O atom [H7···O3 = 2.45 Å, H14···O3 = 2.34 Å] as well as C–H···π interactions involving the C12–C13 bond [H5···(C12–C13)$_\pi$ ≈ 2.6 Å]. The layers are interlinked *via* C–H···O(nitro), C–H···π and H···H short contacts [H15c···O1 = 2.51 Å, H16a···(C4–C5)$_\pi$ ≈ 2.69 Å, H2···H16c = 2.27 Å, respectively] (Fig. 3a). All three of the oxygen atoms engage in multiple close contacts in this structure.

The central ethylene C=C bond in the present 100 K study is substantially longer than that reported by Suh *et al.*[13] from their study at 291 K, and this difference provides a clear indication that there is a temperature dependent disorder of the atoms in the central C=C bond in MMONS-1. This disorder is quite common in stilbenes and related molecules, and for many of the simpler substituted stilbenes and azobenzenes it has been investigated in detail by Ogawa and co-workers using multi-temperature single crystal diffraction data.[22–24] Computational studies on (*E*)-stilbene[25,26] and (*E*)-2,2′-dimethylstilbene,[25] and ^{15}N NMR experiments on crystalline 2′-acetamido-4′-[*N,N*′-bis(2-methoxycarbonyl-ethyl)amino]-4-nitroazobenzene[27] have confirmed that this disorder is dynamic, involving a pedal-like motion of the atoms in the central bond. An important consequence of this motion is the apparent shortening of the central C=C bond length in (*E*)-stilbenes measured at room temperature,

compared to that found at lower temperatures,[22] and the C=C bond length of 1.341(3) Å observed in MMONS-1 agrees well with the value of 1.337(2) Å reported for (*E*)-stilbene at 90 K.[24] However, in contrast to (*E*)-stilbene, where this disorder results in one of the two independent sites in the cell comprising a 95 : 5 ratio of two different conformers even at 90 K, Fourier maps after refinement for MMONS-1 at 100 K reveal no residual peaks in the region of the central C=C bond.‖

MMONS-2

This form crystallizes in the polar noncentrosymmetric space group $P2_1$ with $Z = 4$. Analogous to (*E*)-stilbene, the structure consists of two crystallographically independent molecules in the asymmetric unit, which we label sites 1 and 2. The molecule at site 1 (*molecule 1*) is ordered, whereas site 2 exhibits substantial disorder, being occupied by two different conformers with occupancies of 68% (*molecule 2a*) and 32% (*molecule 2b*) (see Fig. 2 and the torsion angles in Table 2). Molecules 1 and 2a have a similar conformation to the molecule in MMONS-1 while molecule 2b has a different conformation (Fig. 1 and 2); in essence the central –CH=CH– group is disordered over two sites, and this is seen most clearly in Fig. 4b, where the two molecules at site 2 are overlaid. Molecule 1 deviates slightly from planarity, whereas molecules 2a and 2b are essentially planar (see dihedral angles in Table 2). Ogawa's results for substituted stilbenes and azobenzenes demonstrate that the populations of the two conformers at a disordered site are temperature dependent, and also dependent on the specific molecule and its environment. For example, the two orientations in (*E*)-stilbene have relative populations of 85 : 15 at 300 K and 95 : 5 at 90 K, while for azobenzene the relative populations are 82 : 18 and 100 : 0 for the same two temperatures.[24] The azobenzene dye, the subject of solid state NMR experiments in ref. 27, is more structurally similar to MMONS, and that work reported relative populations of 47 : 53 at 293 K and 53 : 47 at 150 K, indicating much less temperature dependence. One polymorph of MOHNS also exhibits disorder of the central C=C bond at room

‖ Residual Fourier electron density maps were produced at the completion of structure refinement. For MMONS-1 there is no sign of additional peaks in the vicinity of the central C7=C8 bond which would indicate a pedal-like disorder of this group of atoms. However, for both MMONS-2 (molecule 1) and MMONS-3 there are small residual peaks in this region, with peak heights less than ∼0.25 e Å^{-3}.

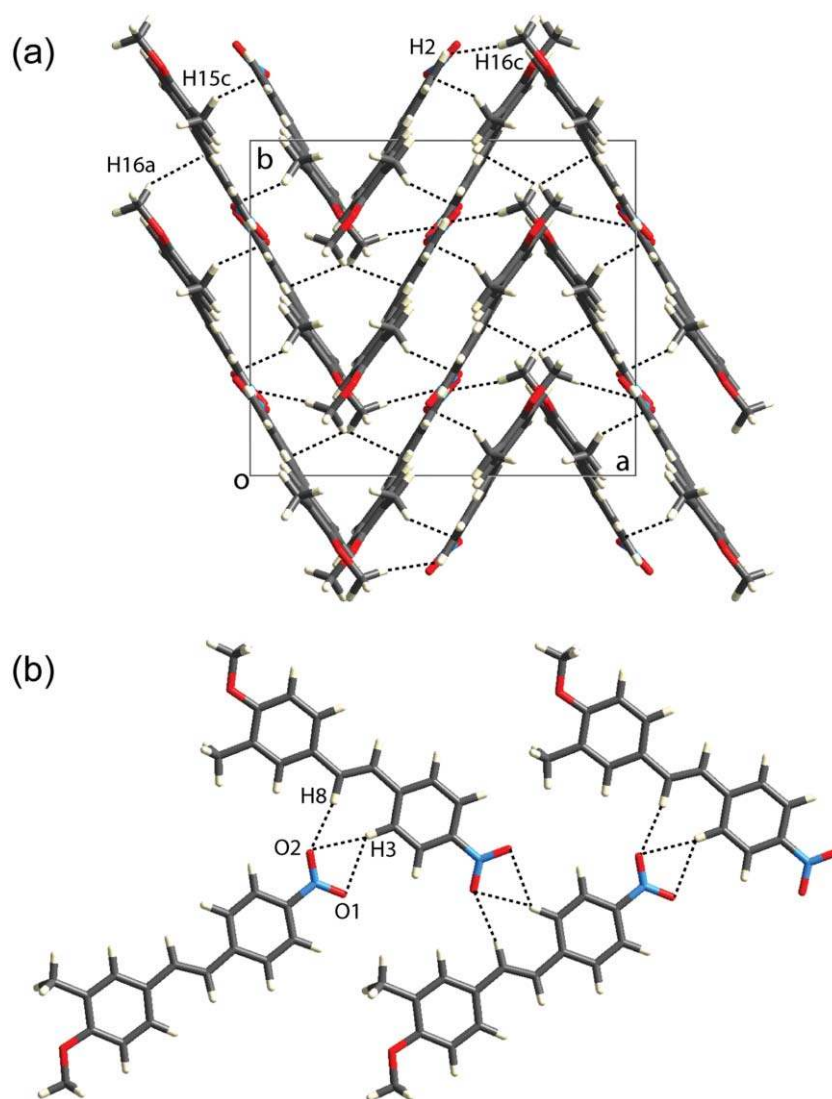**Fig. 3** MMONS-1 (a) Molecular packing diagram viewed down the *c* axis and highlighting C–H···π and H···H close contacts; (b) intermolecular C–H···O close contacts in a sheet.

temperature.[17] No details were reported on relative occupancies of the two conformers, although the disorder was described as static. The crystal structure of MMONS-2 was also determined with a different crystal at 293 K, but relative populations of the two orientations did not change significantly. Thus, we cannot presently conclude whether the disorder at site 2 in MMONS-2 is static or dynamic, although the bulk of evidence for related compounds strongly suggests the latter. A more detailed and precise variable-temperature study seems warranted.

To facilitate discussion of intermolecular contacts in MMONS-2, we examine packing arrangements of two possible hypothetical "ordered" structures: one comprises molecules 1 and 2a, and the other molecules 1 and 2b. Molecule 1 engages in much the same packing arrangement, no matter which of molecules 2a or 2b is assumed to pack with it. However, small and subtle differences are observable. The projection of the structure along [101] in Fig. 4a shows alternating layers of molecule 1 and molecule 2, with the layer formed by molecule 2 being quite narrow compared with the pattern generated by

molecule 1, which interdigitates between alternating molecules at disordered (molecule 2) sites. Interestingly, all three methyl H atoms in molecule 1 engage in relatively close C–H···O intermolecular contacts with molecules 2a/2b [H15a···O3a/*b* = 2.49 Å, H15b···O3a/*b* = 2.63 Å, H15c···O1a/*b* = 2.58 Å], but only H15e of the methyl group of molecule 2a does so [H15e···O2 = 2.60 Å]. Molecule 1 engages in slightly different contacts, depending on whether it is adjacent to the 68 or 32% conformer, and these differences are discussed in more detail in the section below on Hirshfeld surface analysis. Both "ordered" structures exhibit a common C–H···π interaction, involving one of the H atoms of the methyl group in molecule 2a or 2b and either the centre of gravity (Cg1) of the methoxy phenyl ring [H16d···Cg1 ≈ 2.5 Å] or the C10–C11–C12 region of molecule 1 [H16g···C$_\pi$ ≈ 2.7 Å].

MMONS-3

This third polymorphic form crystallizes in the orthorhombic centrosymmetric space group *Pbca* with *Z* = 8. The molecular
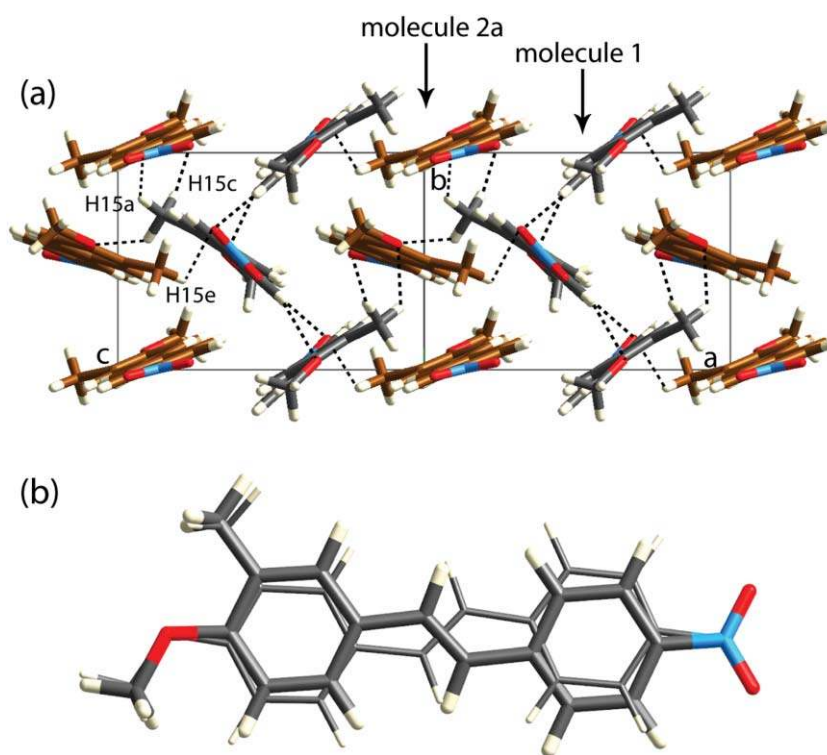
Fig. 4 MMONS-2 (a) Molecular packing diagram viewed along [101] showing close C–H⋯O contacts and molecules at the two different sites in the unit cell. Molecule 1 (grey carbon atoms) is ordered, but two different conformations are disordered at site 2 (only molecule 2a is depicted in the figure, and with brown carbon atoms); (b) Overlay of disordered molecules at site 2; molecule 2a (68% occupancy) is depicted with thick bonds and molecule 2b (32% occupancy) with thin bonds.

ORTEP view (Fig. 1) shows that the molecular conformation in MMONS-3 is similar to molecule 2b in MMONS-2 but distinct from all other molecules of this polymorphic family; MMONS-3 is a clear example of a conformational polymorph. Fig. 2 and Table 2 reveal that the molecule is distinctly non-planar, with a subtle bent geometry; the dihedral angle between the planes of two phenyl rings is 12.8° from X-ray diffraction, and 37.5° after geometry optimization. The molecular packing diagram (Fig. 5a) indicates that the molecules stack along the a axis to form a layered structure. Fig. 5b clearly shows that the crystal structure comprises close intermolecular H⋯H contacts [H16c⋯H6 = 2.21 Å] and C–H⋯O contacts, one involving H7 and O2 [H7⋯O2 = 2.51 Å] and the other across the centre of symmetry, resulting in an end-to-end molecular dimer motif involving the methoxy O atom and H16b of an adjacent methoxy group [H16b⋯O3 = 2.58 Å]. These layers are interlinked *via* close C–H⋯π contacts [H16a⋯C9 = 2.68 Å and H5⋯C11 = 2.74 Å], Fig. 5a. Interestingly, all three methoxy H atoms participate in intermolecular contacts but with different types of acceptors. Further details are explored in the following section.

Comparison between the polymorphs using Hirshfeld surface analysis

The preceding analysis of these three polymorphic crystal structures indicates that they incorporate quite different sets of close intermolecular contacts, and it seems worthwhile quantifying these contacts and hence comparing the polymorphic forms. We have shown recently that tools based on Hirshfeld surfaces are a powerful resource for quantifying intermolecular interactions in molecular crystals,[20] and we apply this approach to the MMONS polymorphs in this section. As a first step we take a "broad brush" approach, and simply sum the areas of all Hirshfeld surface patches that can be identified with each of the various atom—atom contacts, and express these as fractions of the total surface area. Although this approach treats all contacts on an equal footing, both close and more distant, it can be useful to identify gross similarities. The relative contributions obtained in this fashion due to H⋯H, C⋯H, O⋯H and "other" (*i.e.* all of C⋯C, O⋯C, C⋯N, O⋯O, O⋯N, N⋯N and N⋯H) intermolecular contacts are depicted in Fig. 6 for all the molecules in this polymorphic family. In constructing the entries for MMONS-2 we have considered both hypothetical "ordered" structures: molecules 1 and 2a, and molecules 1 and 2b, resulting in four separate Hirshfeld surfaces and corresponding entries in the chart in Fig. 6. This quantitative analysis clearly shows that MMONS-1 contains the highest fraction (42%) of H⋯H contacts but the lowest fraction (21%) of C⋯H (and hence C–H⋯π) contacts. We can also conclude that the patterns of contacts in MMONS-2 and MMONS-3 are broadly similar, but quite different from MMONS-1. Fig. 6 also reveals that the pattern of contacts for molecule 1 of MMONS-2 is essentially independent of which of molecules 2a or 2b are assumed to pack with it in the crystal. In addition, molecules 2a and 2b display almost identical patterns of contacts. A feature common to all molecules in
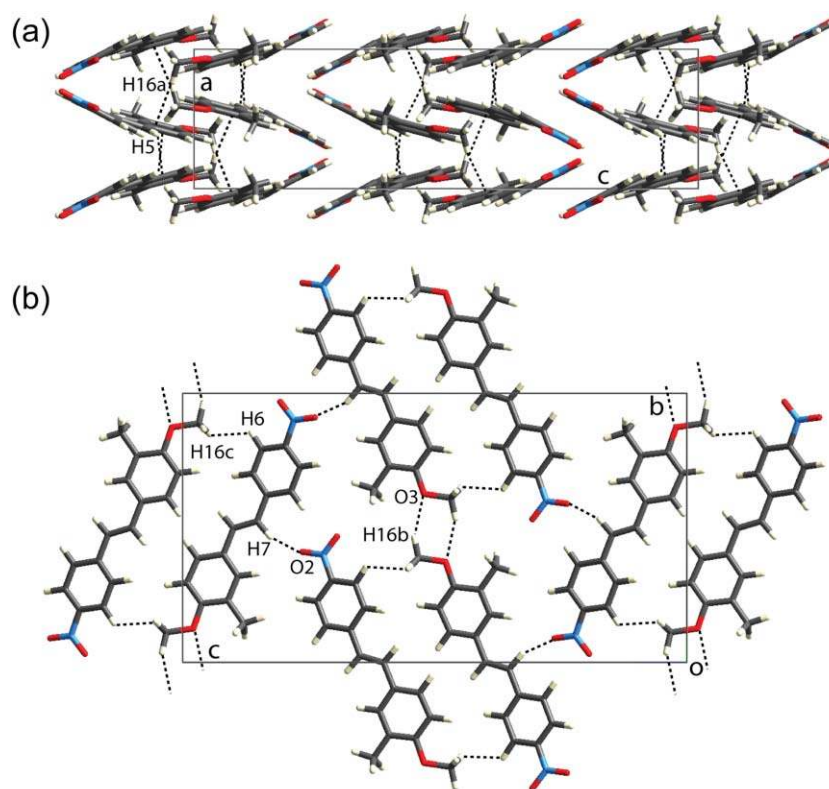
Fig. 5 MMONS-3 molecular packing diagrams (a) viewed down the *b* axis highlighting close C–H···π contacts; (b) down *a* showing close C–H···O and H···H contacts.

these polymorphs is the almost constant fraction of O···H contacts, around 25%.

Fig. 7 and 8 present Hirshfeld surfaces for the molecules in the three polymorphs, and to identify and compare close intermolecular contacts we have mapped the surfaces with d_{norm},[20] a function that highlights contact distances relative to the sum of van der Waals radii, with closest contacts shown in red. For MMONS-1 in Fig. 7 we see three red regions on the left of the surface, reflecting the way in which the molecular sheets intersect *via* C–H···O (involving H7, H14 and O3, Fig. 3) and C5–H5···π contacts. Additional red regions are visible at the top and right of the surface, and these arise from the C–H···O contacts from H3 and H8 to the O(nitro) atoms.

In contrast, the top of the surface for MMONS-3 in Fig. 7 shows only a C–H···π contact from the methyl group, with the closest contacts showing as red regions on the left and lower sides of the surface. Thus, we see in these surfaces the way in which the molecules in MMONS-3 essentially pack in layers with relatively longer contacts between layers, while those in MMONS-1 exhibit close contacts within layers as well as to molecules oriented perpendicular to each layer. MMONS-2 is more difficult to summarize, but separating the disordered structure into two hypothetical "ordered" structures (Fig. 8) is somewhat revealing. Comparing the surfaces for molecule 1 when packed with molecule 2a or with 2b, we see that the close contacts visible as red regions at the bottom edge of the
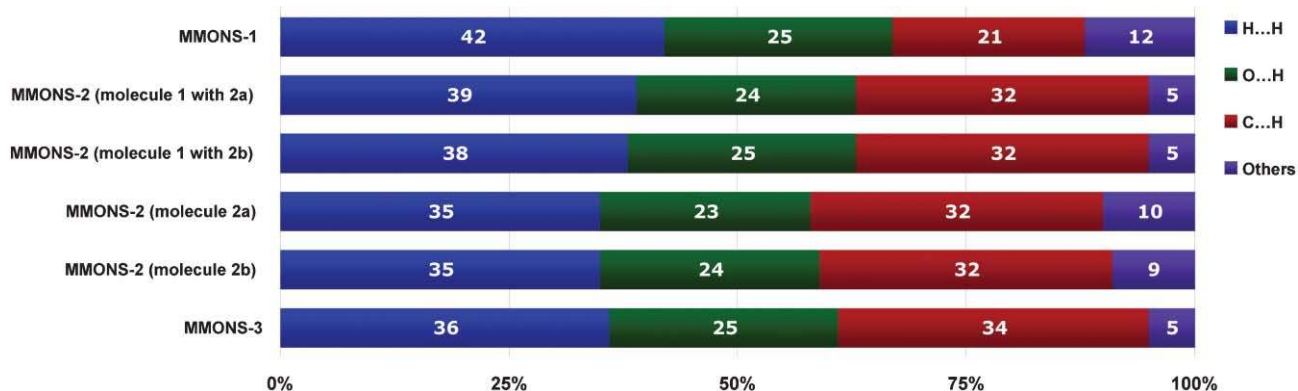

Fig. 6 Relative contributions to the Hirshfeld surface areas for the various intermolecular contacts in the three MMONS polymorphs.
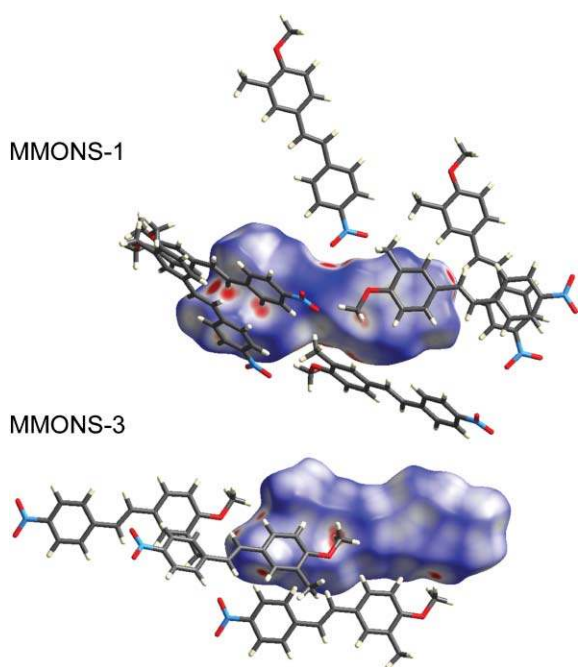
Fig. 7 Hirshfeld surfaces for MMONS-1 and MMONS-3; d_{norm} is mapped on the surfaces over the range −0.15 to 1.1. This function highlights contact distances relative to the sum of van der Waals radii, with closest contacts shown in red.

presence of closer contacts of this kind, but we need to examine many more instances of disorder to be able to draw conclusions such as this. A final comment on these Hirshfeld surface plots concerns the similarity between the surfaces for molecules 2a and 2b, on the right of Fig. 8, and this echoes the nearly identical patterns of contacts seen for these molecules in Fig. 6.

Conclusions

This study has described crystallization experiments for growth of different polymorphic forms of MMONS *via* selection of suitable solvents or mixtures. Two new polymorphs have been discovered and their characterization, along with the low temperature structure of the previously known form, was based on single crystal X-ray diffraction analysis. The polymorphs exhibit two different conformers of this flexible molecule, two of the forms are ordered and involve different conformers, while the third polymorph includes significant disorder involving both conformers at one molecular site. Although all molecules in the crystals are essentially planar, *ab initio* geometry optimizations at the Hartree–Fock level result in two different twisted conformations, with very little energy difference between them (between 0.3 and 1.2 kJ mol^{-1}, depending on the level of theory), evidence of a very flat potential for rotation about the C4–C7 and C8–C9 central bonds. Similarities and differences between the crystalline forms have been elucidated successfully using recently developed Hirshfeld surface-based tools, and we note that this is the first time this approach has been applied to disordered systems of such complexity. The serendipitous discovery of two quite different polymorphic forms for this well-charac-terized NLO material emphasizes the increasing need to undertake quite detailed polymorph screening of all important NLO materials, especially those with significant internal degrees of freedom such as MMONS. Based on the present results, we would be very surprised if further experiments did not reveal additional polymorphic forms. However, our original focus was on MMONS-1, which all available evidence
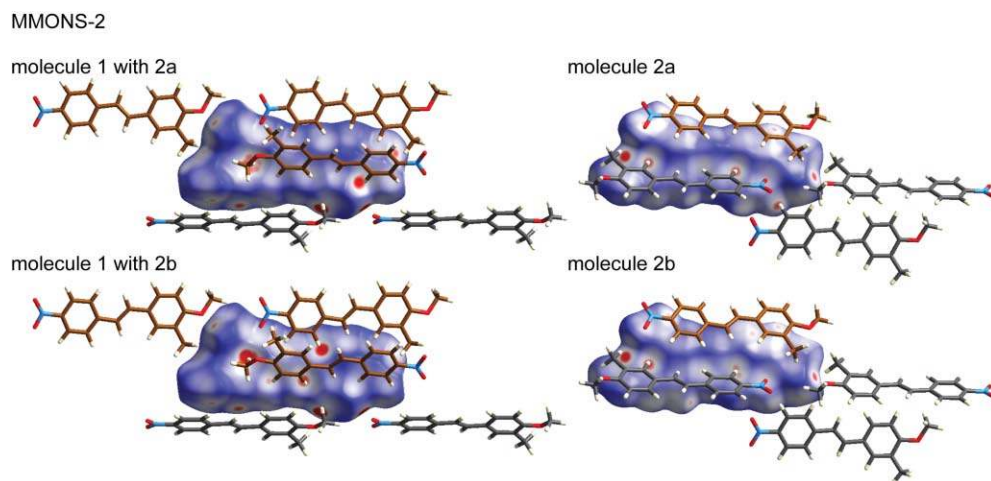
surfaces are unchanged, as these arise from interactions between identical molecules; all changes take place on the upper parts of the surfaces. Replacement of molecule 2a with 2b results in disappearance of the short C5a–H5a···π contact from one adjacent molecule, and appearance of a shorter C3b–H3b···π contact from a different molecule. In addition, existing red regions due to the methyl-H and C14a–H14a contacts with the surface are considerably enhanced, indicating substantially closer contacts of this kind between molecule 1 and 2b, compared with 1 and 2a. It is tempting to attribute the lesser population of molecule 2b at this disordered site to the

Fig. 8 Hirshfeld surfaces for molecules in MMONS-2; d_{norm} is mapped on the surfaces over the range −0.15 to 1.1. Two hypothetical "ordered" structures are considered: molecule 1 with 2a, and molecule 1 with 2b, and each gives rise to two separate Hirshfeld surfaces for each molecule. As for Fig. 4, molecule 1 is depicted with grey C atoms, and molecules 2a and 2b with brown C atoms.

reveals to be completely ordered, and we are currently in the process of analysing high-resolution charge density data for this NLO material.

X-Ray crystallography

High-resolution single-crystal X-ray diffraction data were collected using an Oxford Diffraction Xcalibur diffractometer fitted with a Mo Kα (λ = 0.71073 Å) source. Structures were solved by direct methods using SIR2004[29] and refined by full matrix least squares based on F^2 using SHELXL97.[30] Positions of all hydrogen atoms were fixed at standard neutron geometry (C–H = 1.083 Å)[31] and refined isotropically as riding mobile atoms. All non-hydrogen atoms were refined anisotropically with the exception of one of the molecules in MMONS-2, which has two molecules in the asymmetric unit, one of them disordered over two orientations with occupancies of 0.681 (68%, molecule 2a) and 0.319 (32%, molecule 2b) at 100 K. In the disorder model, the overlapping O and N atoms of the two orientations were refined anisotropically and constrained to share the same positional coordinates and displacement parameters but with respective occupation factors. All carbon atoms of the two orientations were refined isotropically and without constraints. Geometrical calculations were performed using the WinGX[32] program suite, and all packing diagrams and Hirshfeld surface figures and relevant data were obtained with CrystalExplorer.[33]

Theoretical calculations

Single-point calculations were performed at both molecular conformations observed experimentally and, using these as starting geometries, optimizations were performed at the HF/6-31G(d,p) level of theory.[34] Higher-level calculations (B3LYP and MP2) were performed at both the experimental geometries as well as these optimized structures to gain an appreciation for the energy difference between the observed conformers.

Acknowledgements

References

1 C. Bosshard, R. Spreiter, U. Meier, I. Liakatas, M. Bösch, M. Jäger, S. Manetta, S. Follonier and P. Günter, in *Crystal Engineering: From Molecules and Crystals to Materials*, ed. D. Braga, F. Grepioni and A. G. Orpen, Kluwer Academic, Dordrecht, 1999, pp. 261–278; C. Bosshard, K. Sutter, P. Prêtre, J. Hulliger, M. Flörsheimer, P. Kaatz and P. Günter, *Organic Nonlinear Optical Materials*, Gordon and Breach, Basel, 1995; R. L. Sutherland, *Handbook of Nonlinear Optics*, Marcel Dekker, New York, 1996; J. Zyss, *Molecular nonlinear optics. Materials, physics and devices*, Academic Press, New York, 1994; J. Zyss and D. S. Chemla, in *Nonlinear optical properties of organic molecules and crystals*, ed. D. S. Chemla and J. Zyss, Academic Press, London, 1987, vol. 1, pp. 23–191; T. Verbiest, S. Houbrechts, M. Kauranen, K. Clays and A. Persoons, *J. Mater. Chem.*, 1997, **7**, 2175–2189.
2 Y. Wang, W. Tam, S. H. Stevenson, R. A. Clement and J. C. Calabrese, *Chem. Phys. Lett.*, 1988, **148**, 136–141.
3 W. Tam, B. Guerin, J. C. Calabrese and S. H. Stevenson, *Chem. Phys. Lett.*, 1989, **154**, 93–96.
4 J. D. Bierlein, L. K. Cheng, Y. Wang and W. Tam, *Appl. Phys. Lett.*, 1990, **56**, 423–425.
5 R. Kremer, A. Boudrioua, J. C. Loulergue and A. Iltis, *J. Opt. Soc. Am. B*, 1999, **16**, 83–89.
6 S. Tan, A. K. Bhowmik, S. Sodah and M. Thakur, *Appl. Phys. Lett.*, 2000, **77**, 827–829.
7 L. T. Cheng, W. Tam, S. H. Stevenson, G. R. Meredith, G. Rikken and S. R. Marder, *J. Phys. Chem.*, 1991, **95**, 10631–10643.
8 K. Wu, J. Li, C. Lin, C. Mang and B. Zhuang, *Appl. Phys. A*, 2003, **76**, 427–431.
9 S. K. Pan and N. Lei, *Cryst. Res. Technol.*, 1995, **30**, K27–K31; J. W. Park, H. K. Hong, K. S. Lee and C. S. Yoon, *Cryst. Growth Des.*, 2006, **6**, 2011–2020.
10 H. K. Hong, J. W. Park, K. S. Lee and C. S. Yoon, *J. Cryst. Growth*, 2005, **277**, 509–517.
11 K. Komatsu, H. Nanjo, Y. Yamagishi and T. Kaino, *Thin Solid Films*, 2001, **393**, 1–6.
12 A. E. Whitten, D. Jayatilaka and M. A. Spackman, *J. Chem. Phys.*, 2006, **125**, 174505.
13 I. H. Suh, S. S. Lim, J. H. Lee, B. Y. Ryu, M. B. Kim, C. S. Yoon, H. K. Hong and K. S. Lee, *Acta Crystallogr., Sect. C*, 1994, **50**, 1768–1770.
14 Z. M. Jin, Z. Jin and F. Huang, *Powder Diffr.*, 1997, **12**, 136–137.
15 R. M. Vrcelj, E. E. A. Shepherd, C. S. Yoon, J. N. Sherwood and A. R. Kennedy, *Cryst. Growth Des.*, 2002, **2**, 609–617.
16 J. Bernstein, *Polymorphism in Molecular Crystals*, Clarendon Press, Oxford, 2002.
17 A. Gleixner, J. Hiller, T. Debaerdemaeker, A. Lentz and L. Walz, *Z. Kristallogr.*, 1998, **213**, 411–415.
18 F. Pan, C. Bosshard, M. S. Wong, C. Serbutoviez, K. Schenk, V. Gramlich and P. Gunter, *Chem. Mater.*, 1997, 1328–1334; C. B. Aakeröy, A. M. Beatty, M. Nieuwenhuyzen and M. Zou, *J. Mater. Chem.*, 1998, **8**, 1385–1389; T. V. Timofeeva, V. N. Nesterov, R. D. Clark, B. Penn, D. Frazier and M. Y. Antipin, *J. Mol. Struct.*, 2003, **647**, 181–202; D. S. Yufit, O. V. Chetina and J. A. K. Howard, *J. Mol. Struct.*, 2006, **784**, 214–221.
19 J. J. McKinnon, M. A. Spackman and A. S. Mitchell, *Acta Crystallogr., Sect. B*, 2004, **60**, 627–668; M. A. Spackman and J. J. McKinnon, *CrystEngComm*, 2002, **4**, 378–392.
20 J. J. McKinnon, D. Jayatilaka and M. A. Spackman, *Chem. Commun.*, 2007, 3814–3816.
21 L. J. Farrugia, *J. Appl. Crystallogr.*, 1997, **30**, 565–567.
22 K. Ogawa, T. Sano, S. Yoshimura, Y. Takeuchi and K. Toriumi, *J. Am. Chem. Soc.*, 1992, **114**, 1041–1051.
23 J. Harada, K. Ogawa and S. Tomoda, *Acta Crystallogr., Sect. B*, 1997, **53**, 662–672; J. Harada and K. Ogawa, *J. Am. Chem. Soc.*, 2001, **123**, 10884–10888; J. Harada and K. Ogawa, *Top. Stereochem.*, 2006, **25**, 31–47.
24 J. Harada and K. Ogawa, *J. Am. Chem. Soc.*, 2004, **126**, 3539–3544.
25 S. Galli, P. Mercandelli and A. Sironi, *J. Am. Chem. Soc.*, 1999, **121**, 3767–3772.
26 N. A. Murugan and S. Yashonath, *J. Phys. Chem. B*, 2004, **108**, 17403–17411.
27 G. McGeorge, R. K. Harris, A. S. Batsanov, A. V. Churakov, A. M. Chippendale, J. F. Bullock and Z. Gan, *J. Phys. Chem. A*, 1998, **102**, 3505–3513.
28 C. F. Macrae, P. R. Edgington, P. McCabe, E. Pidcock, G. P. Shields, R. Taylor, M. Towler and J. van de Streek, *J. Appl. Crystallogr.*, 2006, **39**, 453–457.
29 M. C. Burla, R. Caliandro, M. Camalli, B. Carrozzini, G. Cascarano, L. De Caro, C. Giacovazzo, G. Polidori and R. Spagna, *J. Appl. Crystallogr.*, 2005, **38**, 381–388.
30 G. M. Sheldrick, *SHELXL97 - Program for crystal structure refinement*, University of Göttingen, Germany, 1997.
31 F. H. Allen, D. G. Watson, L. Brammer, A. G. Orpen and R. Taylor, in *International Tables for Crystallography*, ed. E. Prince, Springer Verlag, Berlin, 3rd edn, 2004, vol. C: Mathematical, physical and chemical tables, pp. 790–811.
32 L. J. Farrugia, *J. Appl. Crystallogr.*, 1999, **32**, 837–838.
33 S. K. Wolff, D. J. Grimwood, J. J. McKinnon, D. Jayatilaka and M. A. Spackman, CrystalExplorer 2.0, (2007) University of

Western Australia (http://hirshfeldsurface.net/CrystalExplorer), Perth.

34 M. J. Frisch, G. W. Trucks, H. B. Schlegel, G. E. Scuseria, M. A. Robb, J. R. Cheeseman, J. A. Montgomery, T. Vreven, K. N. Kudin, J. C. Burant, J. M. Millam, S. S. Iyengar, J. Tomasi, V. Barone, B. Mennucci, M. Cossi, G. Scalmani, N. Rega, G. A. Petersson, H. Nakatsuji, M. Hada, M. Ehara, K. Toyota, R. Fukuda, J. Hasegawa, M. Ishida, T. Nakajima, Y. Honda, O. Kitao, H. Nakai, M. Klene, X. Li, J. E. Knox, H. P. Hratchian, J. B. Cross, V. Bakken, C. Adamo, J. Jaramillo, R. Gomperts, R. E. Stratmann, O. Yazyev, A. J. Austin, R. Cammi, C. Pomelli, J. W. Ochterski, P. Y. Ayala, K. Morokuma, G. A. Voth, P. Salvador, J. J. Dannenberg, V. G. Zakrzewski, S. Dapprich, A. D. Daniels, M. C. Strain, O. Farkas, D. K. Malick, A. D. Rabuck, K. Raghavachari, J. B. Foresman, J. V. Ortiz, Q. Cui, A. G. Baboul, S. Clifford, J. Cioslowski, B. B. Stefanov, G. Liu, A. Liashenko, P. Piskorz, I. Komaromi, R. L. Martin, D. J. Fox, T. Keith, M. A. Al-Laham, C. Y. Peng, A. Nanayakkara, M. Challacombe, P. M. W. Gill, B. Johnson, W. Chen, M. W. Wong, C. Gonzalez and J. A. Pople, Gaussian 03, Revision C.02, Gaussian, Inc., Wallingford, CT, 2004.

35 Z. Li, K. Wu, G. Su and Y. He, *Opt. Mater.*, 2002, **20**, 295–299.

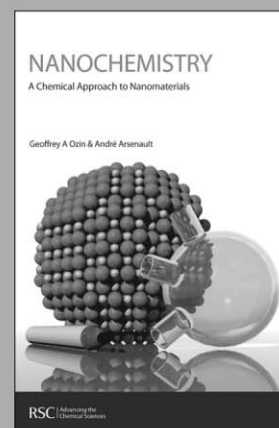36 Z. Li and G. Su, *Acta Crystallogr., Sect. C*, 1995, **51**, 311–313.